Langmuir

INVITED FEATURE ARTICLE

pubs.acs.org/Langmuir

Fast and Stable Photochromic Oxazines for Fluorescence Switching

Erhan Deniz,[†] Massimiliano Tomasulo,[†] Janet Cusido,[†] Salvatore Sortino,[*,‡] and Françisco M. Raymo[*,†]

[†]Laboratory for Molecular Photonics, Department of Chemistry, University of Miami, 1301 Memorial Drive, Coral Gables, Florida 33146-0431, United States

[‡]Laboratory of Photochemistry, Department of Drug Sciences, University of Catania, viale Andrea Doria 6, Catania, I-95125, Italy

Supporting Information

ABSTRACT: The stringent limitations imposed by diffraction on the spatial resolution of fluorescence microscopes demand the identification of viable strategies to switch fluorescence under optical control. In this context, the photoinduced and reversible transformations of photochromic compounds are particularly valuable. In fact, these molecules can be engineered to regulate the emission intensities of complementary fluorophores in response to optical stimulations. On the basis of this general design logic, we assembled a functional molecular construct consisting of a borondipyrromethene fluorophore and a nitrospiropyran photochrome and demonstrated that the emission of the former can be modulated with the interconversion of the latter. This fluorophore−photochrome dyad, however, has a slow switching speed and poor fatigue resistance. To improve both parameters, we developed a new family of photochromic switches based on the photoinduced opening and thermal closing of an oxazine ring. These compounds switch back and forth between ring-closed and -open isomers on nanosecond−microsecond timescales and tolerate thousands of switching cycles with no sign of degradation. In addition, the attachment of appropriate chromophoric fragments to their switchable oxazine ring can be exploited to either deactivate or activate fluorescence reversibly in response to illumination with a pair of exciting beams. Specifically, we assembled three dyads, each based on either a borondipyrromethene or a coumarin fluorophore and an oxazine photochrome, and modulated their fluorescence in a few microseconds with outstanding fatigue resistance. The unique photochemical and photophysical properties of our fluorophore−photochrome dyads can facilitate the development of switchable fluorophores for superresolution imaging and, ultimately, provide valuable molecular probes for the visualization of biological samples on the nanometer level.

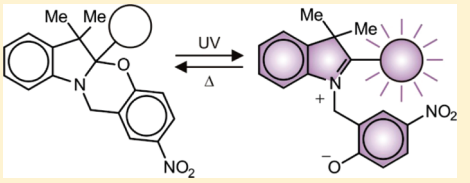

1. INTRODUCTION

The introduction of fluorescent labels[1] within a biological sample offers the opportunity to reconstruct noninvasively an image of the specimen after the excitation of the probes and the collection of their emission with the aid of a microscope.[2] Indeed, fluorescence microscopy is currently the method of choice in the biomedical laboratory for the visualization of cells and tissues.[3] Nonetheless, the phenomenon of diffraction[4] limits the resolution of conventional fluorescence microscopes to hundreds of nanometers in both the horizontal plane and vertical direction.[2] Specifically, fluorescent probes separated by a few nanometers cannot be distinguished in a conventional fluorescence image. Therefore, this convenient technique cannot appreciate the structural details that govern biological processes on the molecular level.

Time can be exploited to resolve what cannot be distinguished in space. In particular, the stringent limitations imposed by diffraction on the spatial resolution of conventional fluorescence microscopes can be overcome with a combination of switchable probes and multiphoton illumination schemes.[5−12] Indeed, labels designed to turn their fluorescence from on to off, or vice versa, in response to optical stimulations permit the temporal resolution of spatially indistinguishable objects and the sequential reconstruction of subdiffraction images. In fact, these clever operating principles to avoid diffraction can extend the resolving power of fluorescence imaging down to the nanoscale. Nonetheless, these strategies require viable mechanisms to switch fluorescence under optical control to allow a transition from microscopy to nanoscopy.

Photochromic compounds[13−18] switch reversibly between states with distinct absorption spectra in the visible region. In some instances, their photoinduced changes in absorption are also accompanied by changes in emission.[18−20] Specifically, only one of the two interconverting states of a photochromic compound is often fluorescent.[21−25] Under these conditions, the photoinduced interconversion of the two states translates into fluorescence switching. Alternatively, the pronounced structural and electronic modifications associated with a photochromic transformation can be engineered to switch the emission of a complementary fluorophore. In particular, fluorescent and photochromic components can be integrated within the same molecular skeleton and the emission of the former can be switched with the photoinduced interconversion of the latter. Indeed, the transformation of one state of the photochromic

Received: March 21, 2011
Revised: May 4, 2011
Published: May 17, 2011

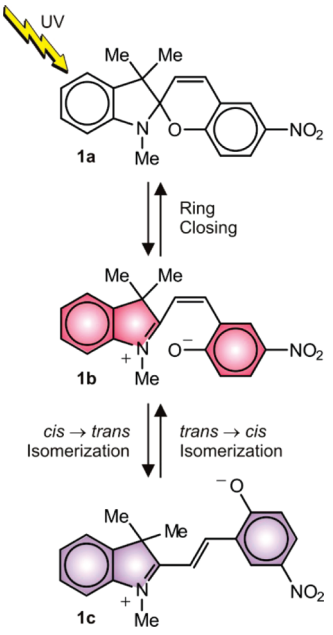

Figure 1. Ultraviolet (UV) illumination of nitrospiropyran **1a** results in the cleavage of the [C−O] bond at the spirocenter to form ring-open intermediate **1b** and the cis → trans isomerization of the adjacent [C═C] bond to generate final merocyanine **1c**. In turn, photogenerated isomer **1c** thermally reverts back to original species **1a** through the same intermediate, **1b**, after trans → cis isomerization and ring-closing steps.

component into the other can either activate or prevent an intercomponent quenching pathway. Under these conditions, the interconversion of the two states of the photochromic component controls the excitation dynamics of the fluorescent partner and modulates its emission intensity. In most fluorophore−photochrome constructs, either electron[26−29] or energy[30−35] transfer is responsible for quenching.[36] In one instance, an electron is transferred either to or from the excited fluorophore from or to, respectively, only one of the two states of the photochrome. This mechanism requires either the oxidation or the reduction potential, respectively, of the photochrome to change significantly with the photochromic transformation. In the other instance, energy is transferred from the excited fluorophore to only one of the two states of the photochrome. This strategy demands the overlap between the emission band of the former and the absorption band of the latter to change significantly with the photochromic conversion. When at least one of these conditions is satisfied, the photochromic transformation translates into fluorescence switching.

Diverse structural designs have been explored over the past six decades to implement photochromic transformations, and numerous families of photochromic molecules have emerged as a result.[13−18] In particular, the photochromism of spiropyrans has been extensively investigated and these compounds are now routinely integrated within a wealth of photoresponsive molecular and supramolecular constructs.[37−48] Synthetic accessibility and reliable photochemical response are the main reasons behind the success of these versatile photoresponsive building blocks. In particular, spiropyrans with a nitro group on their benzopyran fragment (e.g., **1a** in Figure 1) can be prepared from 2-hydroxy-5-nitrobenzaldehyde in a single synthetic step with good yields. Their spirocenter holds the two heterocycles in an orthogonal arrangement and prevents electronic communication between

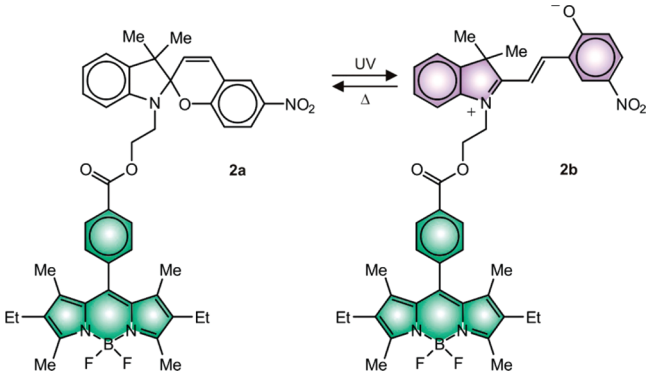

Figure 2. UV irradiation of **2a** converts its nitrospiropyran component to the corresponding merocyanine. In resulting isomer **2b**, the transfer of either an electron or energy from the excited borondipyrromethene to the merocyanine fragment quenches the fluorescence of the former.

the two aromatic chromophores in the ground state (S_0). As a consequence, electronic transitions from S_0 to the first singlet excited state (S_1) of these compounds are generally centered in the ultraviolet region. Upon illumination within this range of wavelengths, however, nitrospiropyrans switch to merocyanine isomers (e.g., **1c** in Figure 1) with good quantum yields. The extended chromophoric system within the photogenerated species absorbs in the visible region, and hence these photoinduced processes result in the appearance of color. In most instances, the photogenerated isomer reverts thermally to the original one with first-order kinetics over the course of hundreds of seconds in organic solvents. Indeed, the photoinduced coloration and thermal decoloration of materials doped with nitrospiropyrans can easily be achieved simply by turning an ultraviolet illumination source on and off.

2. FLUORESCENCE SWITCHING WITH A FLUOROPHORE−PHOTOCHROME DYAD

The significant absorbance changes in the visible region, associated with the photoinduced transformation of a nitrospiropyran to the corresponding merocyanine, can be exploited to activate an energy-transfer pathway and control the emission of a fluorescent partner. On the basis of these considerations, we envisaged the possibility of pairing a borondipyrromethene fluorophore and a nitrospiropyran photochrome within the same molecular construct in the form of compound **2a** (Figure 2).[49] We prepared this molecule in a single synthetic step from preformed borondipyrromethene and nitrospiropyran precursors with pendant carboxylic acid and 2-hydroxyethyl groups, respectively. In particular, the condensation of these two species, under the assistance of 4-dimethylaminopyridine and *N*,*N*′-dicyclohexylcarbodiimide, produced fluorophore−photochrome dyad **2a** with a yield of 54%.

The steady-state absorption spectrum of **2a** (a in Figure 3) is essentially the sum of those of its two separate chromophoric components.[49a] These observations are indicative of negligible electronic interactions between the fluorescent and photochromic fragments of **2a** in S_0. Specifically, the spectrum of **2a** shows a band at 523 nm for the borondipyrromethene fluorophore and one at 347 nm for the nitrospiropyran photochrome. The selective excitation of the fluorescent fragment at 480 nm results in the appearance of its characteristic fluorescence at

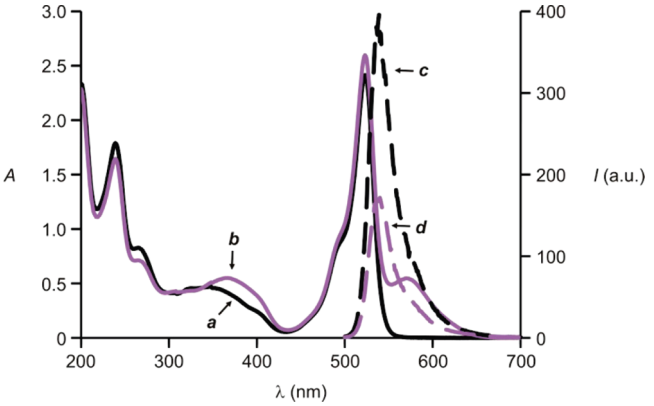

Figure 3. Absorption spectra (0.1 mM, MeCN, 25 °C) of a solution of **2a** recorded (a) before and (b) after ultraviolet illumination (254 nm, 0.5 mW cm^{-2}, 5 min), revealing the appearance of a band at 570 nm for the merocyanine component of photogenerated isomer **2b**. The corresponding emission spectra (0.01 mM, MeCN, 25 °C, 480 nm), recorded (c) before and (d) after irradiation, show a decrease in the borondipyrromethene fluorescence at 539 nm with the photoinduced isomerization.

539 nm in the emission spectrum (c in Figure 3). Indeed, the lack of any overlap between the emission of the fluorophore and the absorption of the photochrome prevents the transfer of energy from the former to the latter and permits the radiative deactivation of the excited borondipyrromethene. Upon ultraviolet illumination, however, the nitrospiropyran switches to the corresponding merocyanine to form **2b** (Figure 2) with the concomitant appearance of its characteristic absorption (b in Figure 3) in the same range of wavelengths where the fluorophore emits. The significant overlap between the absorption of one and the emission of the other permits the transfer of energy from the fluorescent to the photochromic fragment. In addition, the oxidation and reduction potentials of the separate components indicate that the transfer of one electron from the excited fluorophore to the photochrome becomes exergonic with the conversion of the nitrospiropyran to the corresponding merocyanine. Thus, the photochromic transformation activates both electron- and energy-transfer pathways that ultimately encourage the nonradiative deactivation of the excited fluorophore. In fact, the emission intensity recorded for the photostationary state (d in Figure 3) is significantly lower than that measured before ultraviolet illumination (c in Figure 3). Photogenerated state **2b**, however, has a lifetime of 270 s and eventually reverts back to original isomer **2a**. As a result, the initial absorption and emission spectra are fully restored on a timescale of minutes.

The photochemical and photophysical properties of **2a** offer the opportunity to confine fluorescence spatially with patterned illumination.[49b] Indeed, the spin coating of a dichloromethane solution of poly(methyl methacrylate) and **2a** on the surface of a glass slide results in the entrapment of the fluorophore–photochrome dyad within a micrometer-thick polymer film. The illumination of the doped film with a laser, designed to generate a doughnut-shaped pattern with a wavelength of 351 nm, encourages the conversion of **2a** to **2b** exclusively within the irradiated area. Under these conditions, the subsequent illumination at the excitation wavelength of the borondipyrromethene component reveals a dark doughnut-shaped pattern (Figure 4) within the fluorescent film. The thermal reisomerization

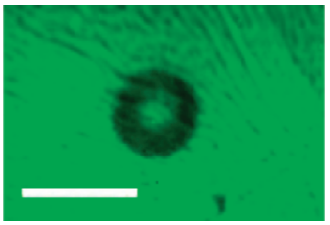

Figure 4. Illumination of a poly(methyl methacrylate) film doped with fluorescent species **2a**, with a laser producing a doughnut-shaped pattern at 351 nm, generating nonfluorescent state **2b** in the illuminated area. As a result, the subsequent excitation at 480 nm reveals a doughnut-shaped nonfluorescent pattern in the corresponding image (scale bar = 1 mm).

of **2b** back to **2a** within the polymer film, however, is relatively slow, and the imprinted pattern fades only after tens of minutes. Furthermore, the emission intensity of the doped film drops to ca. 60% of the initial value after only five switching cycles because of the gradual photodegradation of the dopant. In fact, the slow switching speed and poor fatigue resistance of this fluorophore–photochrome dyad prevent the reconstruction of fluorescence images with subdiffraction resolution, even though the operating principles engineered into this functional molecular construct permit the spatial confinement of fluorescence. Thus, both the speed and the stability of this particular system are in need of significant improvements.

3. IMPROVING THE SPEED AND STABILITY OF THE PHOTOCHROMIC COMPONENT

The nitro group on the benzopyran fragment of nitrospiropyrans promotes intersystem crossing and facilitates their photoinduced isomerization.[50] In particular, the ultraviolet illumination of nitrospiropyran **1a** eventually populates its first triplet state (T_1) and encourages the cleavage of the [C–O] bond at the spirocenter. This process results in the formation of ring-open intermediate **1b** (Figure 1) in T_1 on a picosecond timescale.[51–55] This species can first undergo a cis → trans isomerization along the potential energy surface of T_1 and then decay down to S_0 with the formation of final merocyanine **1c** on a microsecond timescale. Alternatively, it can first decay to S_0 and then undergo a cis → trans isomerization along the potential energy surface of S_0 to form **1c**, once again, in microseconds. Thus, the photoinduced coloration of a nitrospiropyran involves essentially two main chemical steps, occurring on picosecond (ring opening) and microsecond (cis → trans isomerization) timescales respectively.

The participation of T_1 in the isomerization of nitrospiropyrans facilitates the formation of the corresponding merocyanines but also tends to encourage degradation.[56] In fact, the photoinduced conversion of **1a** to **1c** is accompanied by the sensitization of significant amounts of singlet oxygen ($^1\Delta_g$).[50f,g] This species is a strong oxidant, and its production encourages the gradual oxidative degradation of the photochromic system with a depressive effect on its fatigue resistance. Consistently, the fatigue resistances of nitrospiropyrans increase considerably in the presence of singlet oxygen scavengers.[57,58] In principle, the generation of singlet oxygen could be avoided by either drastically reducing the lifetime of T_1 or avoiding its participation in the isomerization process altogether.

Photogenerated merocyanine **1c** spontaneously reverts back to nitrospiropyran **1a** along the potential energy surface of S_0, once again, after two main chemical steps.[50c,e,f] First, the

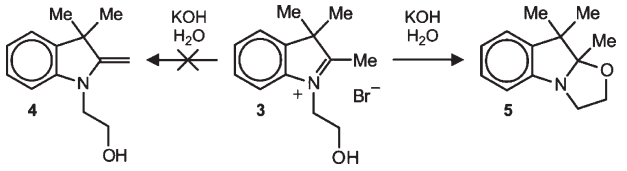

Figure 5. Treatment of the bromide salt of 3*H*-indolium cation **3** with potassium hydroxide to generate 2*H*,4*H*,5*H*-oxazole **5** instead of expected tautomer **4**.

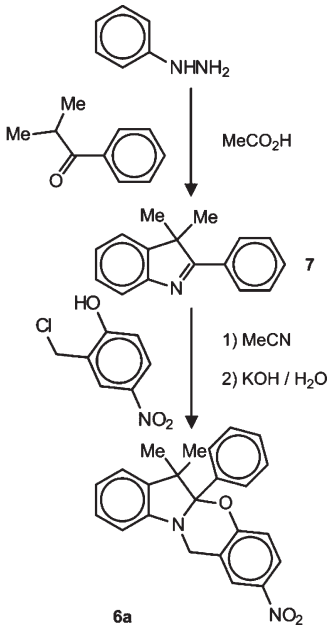

Figure 6. Condensation of phenylhydrazine and *i*-propylphenylketone to generate 3*H*-indole **7** and the reaction of this species with 2-chloromethyl-4-nitrophenol to produce oxazine **6a**.

trans → cis isomerization of the [C═C] double bond joining the cationic and anionic fragments of **1c** produces the intermediate **1b**. Then, the [C−O] bond at the spirocenter reforms to close the benzopyran ring and regenerate **1a**. The first of these two steps, however, is relatively slow and determines the decoloration rate.[59] Specifically, it imposes a lifetime of several hundreds of seconds on **1c** in organic solvents.[50c,e,f] Thus, both the photoinduced coloration and the thermal decoloration of these photochromic compounds are slowed down by the need to change the configuration of a [C═C] bond from cis to trans and trans to cis. In principle, however, the cleavage and reformation of the [C−O] bond at the spirocenter should be sufficient to ensure the pronounced absorbance changes in the visible region expected from photochromic transformations. Therefore, photochromic switches faster than conventional nitrospiropyrans could simply be realized by preventing the slow cis/trans isomerization steps and instead relying exclusively on the inherently fast ring-opening and -closing steps.

To synthesize a nitrospiropyran with a 2-hydroxyethyl appendage on its 2*H*,3*H*-indole nitrogen atom, we intended to convert the bromide salt of 3*H*-indolium cation **3** (Figure 5) to 3*H*-indole **4** and condense this compound with 2-hydroxy-5-nitrobenzaldehyde.[60] The treatment of **3** with potassium hydroxide, however, did not produce expected compound **4**. Instead, it resulted in the formation of its tautomer, **5**, after the closing of a

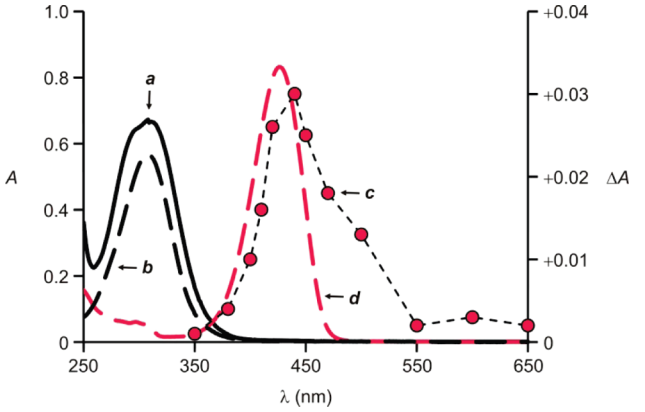

Figure 7. Steady-state absorption spectra (0.1 mM, MeCN, 25 °C) of (a) **6a** and (b) 4-nitroanisole showing essentially the same band for the S_0 absorption of their 4-nitrophenoxy chromophore. (c) The time-resolved absorption spectrum of a solution (0.1 mM, MeCN, 25 °C) of **6a**, recorded 30 ns after illumination with a pulsed laser (355 nm, 6 ns, 8 mJ), and (d) the steady-state absorption spectrum (0.1 mM, MeCN, 25 °C) of *t*-butylammonium 4-nitrophenolate reveal essentially the same band for the S_0 absorption of their 4-nitrophenolate chromophore.

2*H*,4*H*,5*H*-oxazole ring. In light of the structural implications in the isomerization mechanism of nitrospiropyrans, we realized that the introduction of an appropriate chromophore onto the rim of the oxazole ring of **5** would offer the opportunity to implement photochromic transformations based exclusively on fast ring-opening and -closing steps. On the basis of these considerations and the availability of appropriate precursors, we designed 2*H*,4*H*-[1,3]oxazine **6a** (Figure 6) and synthesized this compound in two steps, starting from phenyl hydrazine and *i*-propylphenyl ketone.[61] In particular, the condensation of these two commercial precursors under acidic conditions gave 3*H*-indole **7** in a yield of 76%. The reaction of **7** with 2-chloromethyl-4-nitrophenol produced target molecule **6a** in a yield of 58%.

The steady-state absorption spectrum of **6a** (a in Figure 7) shows a band centered at 308 nm (λ_a in Table 1). This band resembles the absorption of 4-nitroanisole (b in Figure 7) and can be assigned to the 4-nitrophenoxy chromophore of **6a**. Illumination in the tail of this absorption with a pulsed laser operating at 355 nm results in the cleavage of the [C−O] bond at the junction of the two heterocycles and the opening of the oxazine ring with a quantum yield of 0.10 (ϕ in Table 1). This process generates zwitterionic isomer **6b** (Figure 8) within the laser pulse (6 ns) and is accompanied by the appearance of an absorption band centered at 440 nm (λ_b in Table 1 and c in Figure 7). This band resembles the S_0 absorption of *t*-butylammonium 4-nitrophenolate (d in Figure 7) and can be assigned to the anionic chromophore of **6b**. This transient absorption decays monoexponentially on a nanosecond timescale with the spontaneous reisomerization of **6b** back to **6a**.[62] Curve fitting of the temporal absorbance evolution (Figure 9) indicates the lifetime of the photogenerated species to be 22 ns (τ in Table 1).[63] In fact, a full switching cycle, from **6a** to **6b** and back, can be completed in a few tens of nanoseconds. Furthermore, the photoisomerization of **6a** to **6b** is not accompanied by the sensitization of singlet oxygen, as in the case of nitrospiropyrans. As a result, this photochromic system can be switched back and forth between its two states thousands of times without decomposing, even in the presence of molecular oxygen. Thus, the transition from

Table 1. Photochemical and Photophysical Parameters Associated with Oxazines 6a, 9a, 14a, 15a, 17a−20a, 22a, 24a, and 25a[a]

	λ_a (nm)	λ_b (nm)	ϕ	τ	ref
6a	308	440	0.10	22 ns	61
9a	338	510	0.11	29 ns	64c
14a	304	440	0.11	21 ns	65d
15a	310	440	0.01	10 μs	65d
17a	288	420	0.08	38 ns	65a−65c
18a	330	430	0.28	140 ns	65b,65c
19a	305	440 and 550	0.07	2 μs	65d
20a	318	440	0.03	22 ns	61b,61c
22a	305	430 and 560	0.05	1 μs	72
24a	305	430 and 560	0.02	3 μs	72
25a	412	570	0.02	0.2 μs	73

[a] The absorption wavelengths for the ring-closed (λ_a) and -open (λ_b) isomers, the quantum yield (ϕ) of the photoinduced ring-opening process, and the lifetime (τ) of the ring-open isomer were measured by steady-state and time-resolved absorption spectroscopies in MeCN at 20−25 °C. The time-resolved spectra were recorded after excitation at 355 nm with a pulsed Nd:YAG laser (6 ns, 8−12 mJ). The structure of **20a** is shown below.

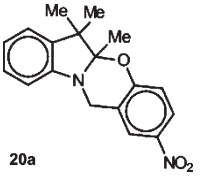

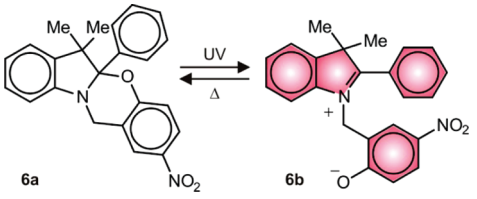

Figure 8. UV illumination of **6a** opens the oxazine ring to form zwitterionic isomer **6b**. In turn, photogenerated isomer **6b** thermally reverts back to the original species, **6a**, after the closing of the oxazine ring.

nitrospiropyran **1a** to oxazine **6a** translates into a decrease in the time required to complete a full switching cycle from hundreds of seconds to only tens of nanoseconds and an increase in the number of switching cycles tolerated by the photochromic system from a few tens to several thousands. The significant improvements in switching speed and fatigue resistance are mostly a consequence of the fact that the photoinduced coloration of **6a** and the thermal decoloration of **6b** do not require cis/trans isomerization steps and are instead exclusively based on ring opening and closing. Thus, the replacement of the nitrospiropyran component of fluorophore−photochrome dyad **2a** with an oxazine similar to **6a** can translate into the needed enhancements in speed and stability. Nonetheless, the absorption properties of the photogenerated isomer of the oxazine must first be optimized to ensure the transfer of energy from

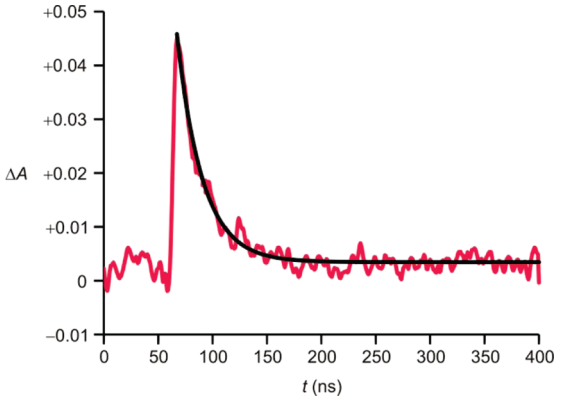

Figure 9. S_0 absorption of the 4-nitrophenolate chromophore of **6b**, detected after the illumination of a solution (0.1 mM, MeCN, 25 °C) of **6a** with a pulsed laser (355 nm, 6 ns, 8 mJ), decaying monoexponentially with the reisomerization of **6b** back to **6a** on a nanosecond timescale.

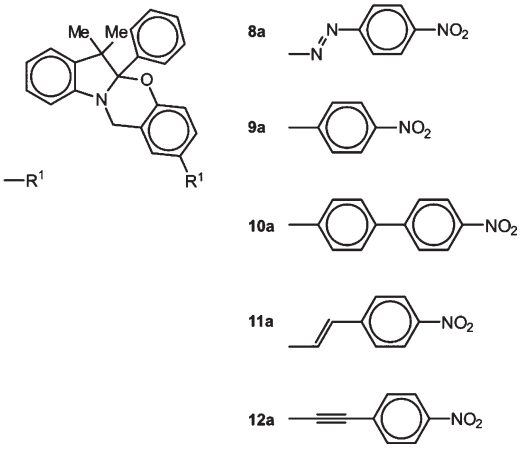

Figure 10. Substituent R^1 on the phenoxy fragment of the oxazine core can be modified, in the form of compounds **8a**−**12a**, to extend the conjugation of this chromophore and, in principle, to regulate the color of the ring-open isomer.

the fluorescent partner integrated within the fluorophore−photochrome dyad.

4. REGULATING THE COLOR OF THE PHOTOCHROMIC COMPONENT

The 4-nitrophenolate anion of zwitterionic isomer **6b** absorbs in the visible region and is responsible for the photoinduced coloration of this particular photochromic system.[61] In acetonitrile, its absorption band is centered at 440 nm (λ_b in Table 1) and, in principle, can be shifted bathochromically by extending the conjugation of this chromophoric fragment. Specifically, the insertion of π systems between the phenoxy ring of **6a** and its nitro group can offer the opportunity to regulate the color of the photogenerated isomer. On the basis of these considerations, we synthesized oxazines **8a**−**12a** (Figure 10), differing in the nature of the substituent (R^1) in the para position relative to the phenoxy oxygen atom.[64] In particular, we isolated **8a**−**12a** in yields ranging from 21 to 51% after the reaction of **7** (Figure 6) with the corresponding 2-bromomethyl-4-R^1-phenol. Instead, we synthesized **11a** and **12a** in yields of 81 and 16% by coupling

4-nitrostyrene and (4-nitrophenyl)acetylene, respectively, with a preformed oxazine having a bromine substituent in the para position relative to the phenoxy oxygen atom.

The steady-state absorption spectra of **8a**−**12a** (Figure S1) show bands for their phenoxy chromophores centered at wavelengths significantly longer than that of parent oxazine **6a**. Specifically, the bathochromic shift relative to **6a**, designed into these chromophores, varies from 30 nm for **9a** to up to 63 nm for **8a**. Excitation within these bands under experimental conditions identical to those employed for **6a**, however, opens the oxazine ring to form the corresponding zwitterionic isomer in S_0 only for **9a**. In particular, **9a** switches to **9b** upon ultraviolet illumination with a quantum yield of 0.11 (ϕ in Table 1). Consistently, a band for the S_0 absorption of the phenolate anion of **9b** appears at 510 nm (λ_b in Table 1) in the spectrum recorded after excitation. The photogenerated isomer has a lifetime of 29 ns (τ in Table 1) and switches back to the original species with first-order kinetics and the monoexponential decay of its absorbance in the visible region. In fact, the photochemical response of this photochromic system is almost identical to that of the parent one, with the exception of the bathochromic shift engineered into the phenoxy and phenolate chromophores of the two interconverting isomers.

The excitation dynamics of **8a** and **10a**−**12a** are, instead, significantly different from those of **6a** and **9a**. Indeed, the time-resolved spectrum of **8a** (a in Figure S2) shows the bleaching of its S_0 absorption upon excitation with the concomitant appearance of a weaker band at shorter wavelengths. These transient absorptions persist for hundreds of microseconds and eventually disappear on millisecond−second timescales. This behavior is consistent with the photoinduced trans → cis isomerization of the 4-nitrophenylazophenoxy chromophore and its subsequent thermal cis → trans reisomerization. In contrast to the behavior of **8a**, the time-resolved absorption spectra of **10a** and **11a** (b and c in Figure S2) reveal the appearance of absorptions upon excitation that decay on a microsecond timescale. The lifetimes of these transient species, however, decrease significantly in the presence of molecular oxygen. Furthermore, their bands resemble those observed upon the excitation of model phenoxy chromophores and can be assigned to T_1 absorptions of **10a** and **11a**. The time-resolved absorption spectrum of **12a** (d in Figure S2) also shows the formation of a transient species upon excitation with a lifetime dependent on the concentration of molecular oxygen. Its band, however, resembles the one observed upon excitation of a model phenolate equivalent to that incorporated within ring-open isomer **12b** and can be assigned to an absorption in the triplet manifold of this species. Thus, the trans → cis isomerization of the phenoxy chromophore of **8a** and the intersystem crossing of the phenoxy chromophores of **10a**−**12a** dominate the excitation dynamics of these systems and, with the exception of **12a**, prevent the opening of the oxazine ring.

The complications associated with the excitation dynamics of **8a** and **10a**−**12a** encouraged us to explore an alternative strategy to regulate the color of the photogenerated isomer. In particular, we realized that, in addition to the anionic fragment, the cationic component of this zwitterionic species also can be designed to absorb in the visible region with the introduction of appropriate substituents. Indeed, the opening of the oxazine ring can extend the conjugation of a chromophore attached to the chiral center at the junction of the two heterocyclic fragments and shift its absorption band bathochromically. On the basis of these considerations, we designed oxazines **13a**−**19a** (Figure 11), differing

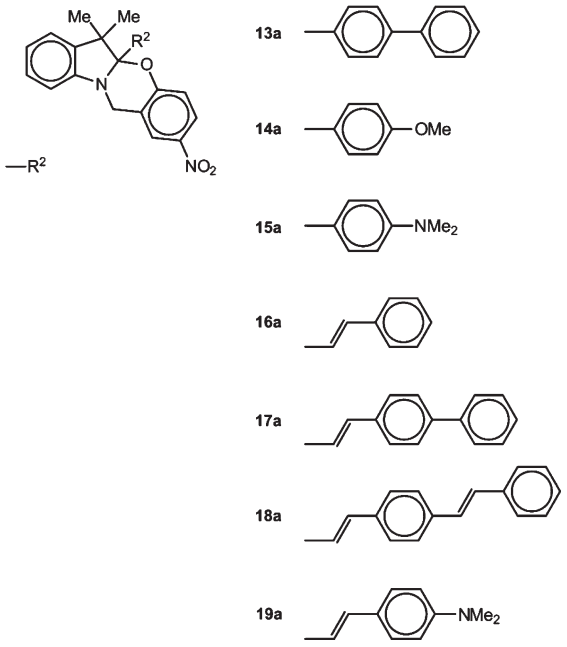

Figure 11. Substituent R^2 on the chiral center of the oxazine ring can be modified, in the form of compounds **13a**−**19a**, to extend the conjugation of the 3*H*-indolium cation generated upon ring opening and, in principle, regulate the color of the ring-open isomer.

in the nature of the substituent (R^2) on the chiral center.[65] By analogy to the synthetic procedure devised for the preparation of **6a** (Figure 6), we isolated **13a**−**15a** in overall yields ranging from 26 to 37% after the condensation of phenylhydrazine with the corresponding *i*-propyl-R^2-ketone and the reaction of the resulting 3*H*-indole with 2-chloromethyl-4-nitrophenol. Instead, we prepared **16a**−**19a** in a single step with yields ranging from 40 to 76%, starting from preformed oxazine **20a** (Table 1) and the aldehyde of the corresponding chromophoric appendage.[66,67] This versatile synthetic approach offers the opportunity to condense a switchable oxazine to virtually any chromophore with a formyl substituent and is definitely a convenient protocol for the preparation of functional molecular constructs.

The steady-state absorption spectra of **13a**−**19a** show a band for the 4-nitrophenoxy chromophore at ca. 310 nm (a in Figure 12).[65] Upon excitation within this band, the oxazine ring of these compounds, with the exception of **13a** and **16a**, opens to form the corresponding zwitterionic isomers with quantum yields ranging from 0.01 to 0.28 (ϕ in Table 1).[68] Consistently, the S_0 absorption of the 4-nitrophenolate anion of the ring-open isomers appears at ca. 440 nm (λ_b in Table 1) in the spectra recorded after excitation. Instead, the time-resolved spectra of **13a** and **16a** do not reveal any significant change upon illumination. In fact, the redox potentials of model fragments suggest that the photoinduced transfer of an electron from R^2 to the nitro group of **13a** and **16a** is exergonic, and presumably, this competitive process prevents the opening of their oxazine ring.[65b]

The photoinduced ring opening of **14a**, **15a**, and **17a**−**19a** brings R^2 into conjugation with the 3*H*-indolium cation of their ring-open isomers. This structural transformation bathochromically shifts the absorption of R^2 and, with the exception of the conversion of **14a** into **14b**,[69] results in the appearance of an additional band in the visible region. In **15b**, **17b**, and **18b**, this

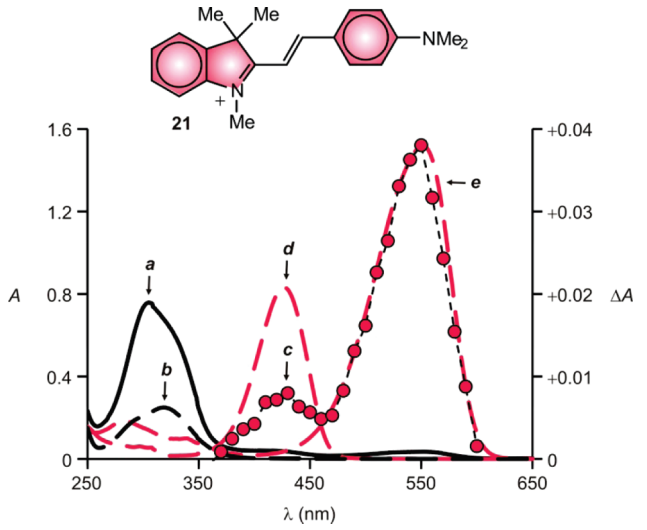

Figure 12. Steady-state absorption spectra (0.05 mM, MeCN, 25 °C) of (a) **19a** and (b) 4-nitroanisole showing essentially the same band for their 4-nitrophenoxy chromophore. (c) The time-resolved absorption spectrum of a solution (0.01 mM, MeCN, 25 °C) of **19a**, recorded 0.1 μs after illumination with a pulsed laser (355 nm, 6 ns, 12 mJ), and the steady-state absorption spectra (0.1 mM, MeCN, 25 °C) of (d) *t*-butylammonium 4-nitrophenolate and (e) the hexafluorophosphate salt of **21** reveal essentially the same band for the S_0 absorptions of the 4-nitrophenolate and 3*H*-indolium chromophores.

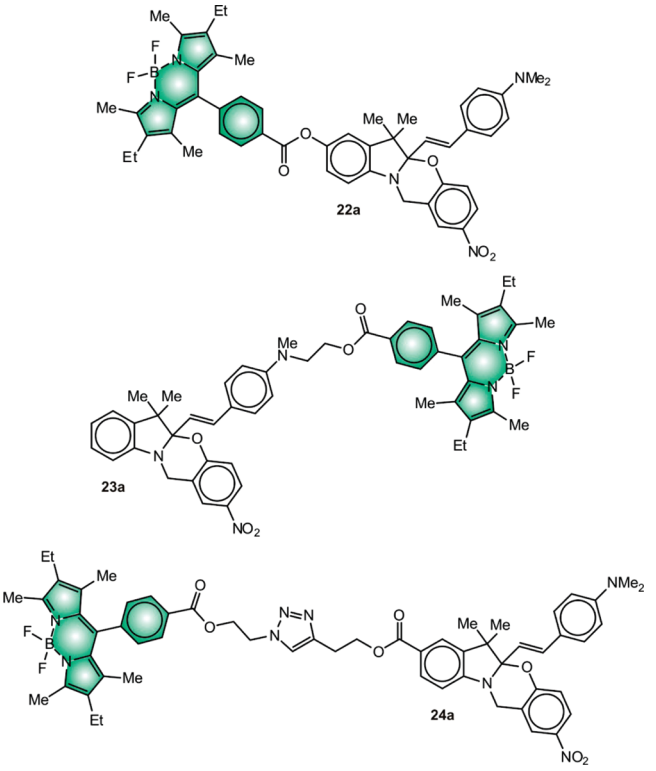

Figure 13. Dyads **22a**−**24a** incorporating a borondipyrromethene fluorophore and an oxazine photochrome and differing in the nature of the covalent linkage bridging the two functional components.

absorption overlaps that of their 4-nitrophenolate anion. In fact, the photoinduced formation of bichromophoric isomers **17b** and **18b** translates into 2- and 7-fold enhancements in the coloration efficiency at 430 nm, respectively, relative to that of parent monochromophoric system **6b**.[70,71] In both instances, the transient absorption decays monoexponentially with the reisomerization of the ring-open to the ring-closed isomer. The lifetime of **15b**, however, is 10 μs (τ in Table 1), whereas those of all of the other ring-open isomers are in the nanosecond domain. Presumably, the ability of the dimethylamino group to donate electrons results in the stabilization of the 3*H*-indolium cation of **15b** with a concomitant delay of the reisomerization kinetics, relative to parent system **6b**.

In **19b**, the cationic and anionic fragments absorb at distinct wavelengths, and consistently, a pair of bands at 440 and 550 nm (λ_b in Table 1) appear in the absorption spectrum (c in Figure 12) recorded upon illumination.[65d] These transient bands resemble the steady-state absorptions (d and e in Figure 12) of *t*-butylammonium 4-nitrophenolate and the hexafluorophosphate salt of model 3*H*-indolium cation **21**, respectively, confirming their assignment. Furthermore, they decay with identical kinetics (a and b in Figure S3), demonstrating that they are both associated with the same species. Specifically, monoexponential fittings of both absorbance evolutions indicate the lifetime of **19b** to be 2 μs (τ in Table 1). Once again, the ability of the dimethylamino group to donate electrons and stabilize the 3*H*-indolium cation of **19b** is presumably responsible for the slower reisomerization kinetics relative to parent system **6b**. In any case, only a few microseconds are sufficient to complete a full switching cycle with this bichromophoric photochrome. Furthermore, this system tolerates hundreds of cycles without decomposing, and the intense absorption of the 3*H*-indolium chromophore within its photogenerated isomer can be exploited to ensure the transfer of energy from a complementary fluorophore. Thus, this particular oxazine is a viable alternative to the nitrospiropyran embedded in **2a** for the realization of fast and stable fluorophore−photochrome dyads.

5. FAST AND STABLE FLUOROPHORE−PHOTOCHROME DYADS

The slow switching speeds and poor fatigue resistance of fluorophore−photochrome dyad **2a** can be improved with the introduction of an oxazine, similar to **19a**, within this molecular construct in place of the nitrospiropyran component.[72] Indeed, the 3*H*-indolium cation of ring-open isomer **19b** absorbs in the same range of wavelengths where the borondipyrromethene fluorophore of **2a** emits. As a result, this particular chromophore can accept the excitation energy of the borondipyrromethene fragment. In addition, the oxidation potential of this fluorophore and the reduction potential of the hexafluorophosphate salt of model 3*H*-indolium cation **21** indicate that the transfer of one electron from the former to the latter upon excitation is exergonic with a free-energy change of −0.5 eV. Thus, both electron- and energy-transfer processes can quench the borondipyrromethene fluorescence, after the photoinduced opening of the oxazine ring, if the two components are integrated within the same molecular skeleton. On the basis of these considerations, we designed fluorophore−photochrome dyads **22a**−**24a** (Figure 14) and synthesized these compounds in three to eight steps from known precursors. These molecules incorporate essentially the same fluorescent and photochromic fragments but differ in the covalent bridge linking the two functional components.

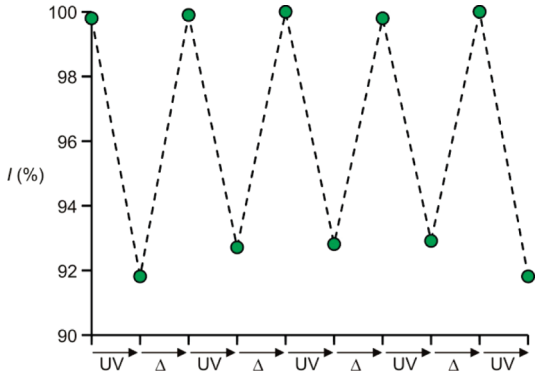

Figure 14. Decrease in the emission intensity (0.01 mM, MeCN, 20 °C, 532 nm) of a solution of **23a** when a UV source (355 nm, 6 ns, 12 mJ) is turned on. The emission intensity returns to its original value when the irradiation source is turned off.

By analogy to the spectroscopic response of **2a**, the steady-state absorption spectra of **22a**−**24a** are approximately the sum of those of their separate fluorescent and photochromic fragments.[72] Once again, these observations are indicative of the lack of electronic interactions between the fluorescent and photochromic components within each dyad in S_0. In all instances, the 4-nitrophenoxy chromophore of the photochromic fragment absorbs at 305 nm (λ_a in Table 1). Excitation within this band opens the oxazine rings of **22a** and **24a** but not that of **23a**, with quantum yields of 0.05 and 0.02, respectively (ϕ in Table 1). The process is accompanied by the appearance of the S_0 absorptions of the 4-nitrophenolate and 3*H*-indolium chromophores of ring-open isomers **22b** and **24b** at 430 and 560 nm, respectively (λ_b in Table 1). Both bands decay monoexponentially with the reisomerization of these species back to the original ring-closed isomers. Curve fittings of the temporal absorbance evolutions indicate the lifetimes of **22b** and **24b** to be 1 and 3 μs, respectively (τ in Table 1). In fact, the behavior of both fluorophore−photochrome dyads upon ultraviolet excitation is almost identical to that of the photochrome **19a**. Thus, the photochromism of the oxazine is essentially unaffected by the covalent attachment of a borondipyrromethene appendage in these particular dyads. In contrast to the behavior of **22a** and **24a**, however, the other dyad, **23a**, does not open its oxazine ring in response to ultraviolet excitation, under otherwise identical conditions. In this instance, the corresponding time-resolved absorption spectrum does not reveal any significant absorbance change in the range of wavelengths where the anionic and cationic fragments of zwitterionic isomer **23b** are expected to absorb.

On the basis of the spectral overlap and redox potentials, the 3*H*-indolium chromophore of photogenerated isomers **22b** and **24b** can quench the fluorescence of the borondipyrromethene component in both dyads.[72] Indeed, the emission intensity of the two fluorophore−photochrome assemblies decreases with the photoinduced ring opening of the photochromic fragment and reverts to the original value in a few microseconds with its thermal ring closing. In fact, their fluorescence can be modulated for hundreds of switching cycles with no sign of degradation simply by turning a beam at 355 nm on and off to operate the photochromic component while illuminating the sample at 532 nm to excite the fluorescent component (Figure 14). Nonetheless, the limited quantum efficiency for the photochromic

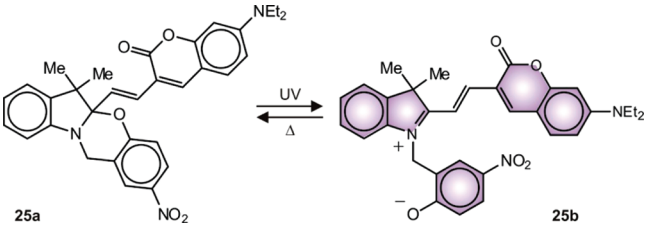

Figure 15. UV illumination of **25a**, which opens the oxazine ring and brings the coumarin fluorophore into conjugation with the 3*H*-indolium cation of photogenerated isomer **25b**.

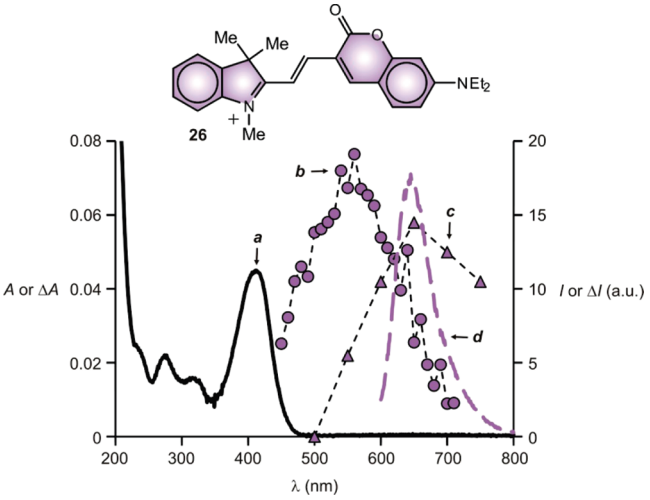

Figure 16. Steady-state (a, 2.5 μM) and time-resolved (b, 0.01 mM, 355 nm, 6 ns, 10 mJ, 0.03 μs) absorption spectra of solutions (MeCN, 20 °C) of **25a** showing S_0 absorptions at 412 and 570 nm respectively for the coumarin fluorophore. The emission spectra of solutions (MeCN, 20 °C) of **25a** (c, 0.01 mM), recorded upon simultaneous illumination at 355 nm (6 ns, 10 mJ) and 532 nm (6 ns, 30 mJ), and of the hexafluorophosphate salt of model 3*H*-indolium cation **26** (d, 2.5 μM), recorded upon excitation at 593 nm, show essentially the same band for the coumarin fluorophore.

transformation translates into modest contrast ratios at moderate illumination intensities for both systems.

In search of strategies to enhance the contrast ratio of our photoswitchable fluorophores, we realized that the mechanism designed into **13a**−**19a** to control color can be adapted to regulate fluorescence as well. Specifically, the ability of a fluorescent fragment, attached to the chiral center at the junction of the two heterocycles, to absorb exciting radiation in the visible region can be controlled by opening and closing the oxazine ring. In turn, the associated change in absorbance at the excitation wavelength of the fluorophore translates into a change in emission intensity. On the basis of these considerations, we designed fluorophore−photochrome dyad **25a** (Figure 15).[73] This compound combines a coumarin fluorophore and an oxazine photochrome into its molecular backbone and can be isolated with a yield of 40% after the condensation of **20a** with a formylated coumarin, under the assistance of trifluoroacetic acid.

The steady-state absorption spectrum (a in Figure 16) of **25a** shows a band at 412 nm (λ_a in Table 1) for the coumarin appendage attached to the oxazine ring.[73] Upon ultraviolet illumination, **25a** switches to **25b** (Figure 15) with a quantum yield of 0.02 (ϕ in Table 1) and a concomitant bathochromic

shift of the absorption of the coumarin fluorophore. Indeed, the ring-opening process brings the fluorescent appendage into conjugation with the 3*H*-indolium cation and shifts its band to 570 nm (λ_b in Table 1 and b in Figure 16). Photogenerated isomer **25b** reverts to ring-closed species **25a** with first-order kinetics on a microsecond timescale. As a result, the absorbance at 570 nm decays monoexponentially with the reisomerization process (Figure S4). Curve fitting of the absorbance evolution indicates the lifetime of **25b** to be 0.2 μs (τ in Table 1).

The pronounced bathochromic shift that accompanies the photoinduced transformation of ring-closed isomer **25a** to ring-open species **25b** can be exploited to activate fluorescence with a virtually infinite contrast ratio.[73] Indeed, the illumination of **25a** at 532 nm does not result in any significant fluorescence, simply because the coumarin appendage of the ring-closed isomer cannot absorb at this particular wavelength. After ring opening, however, the coumarin band shifts sufficiently to permit the absorption of the exciting radiation at 532 nm. Consistently, the emission spectrum (c in Figure 16), recorded upon simultaneous irradiation of the sample at 355 nm to open the oxazine ring and at 532 nm to excite the coumarin fluorophore, shows a band at 650 nm. This band resembles that detected in the steady-state emission spectrum (d in Figure 16) of the hexafluorophosphate salt of model 3*H*-indolium cation **26** and corresponds to the fluorescence of the coumarin fragment of **25b**. In fact, the fluorescence of this particular fluorophore−photochrome dyad can be switched on and off for hundreds of cycles with no sign of degradation simply by turning an irradiation source at 355 nm on and off while illuminating the sample at 532 nm.

6. CONCLUSIONS

The photoinduced conversion of a nitrospiropyran to the corresponding merocyanine can be exploited to switch off the fluorescence of a covalently connected borondipyrromethene and then turn it back on after thermal reisomerization. Indeed, the photoinduced transformation of the photochromic component activates electron- and energy-transfer pathways and results in the effective quenching of the excited fluorophore. The emission photodeactivation in such a fluorophore−photochrome dyad permits the spatial confinement of fluorescence with patterned illumination and, in principle, offers the opportunity to reconstruct images with subdiffraction resolution. Nonetheless, the slow reisomerization kinetics of the photochromic component and its tendency to degrade under illumination impose a poor switching speed and limited fatigue resistance. Both parameters can be improved dramatically simply by eliminating the need for the cis/trans isomerization steps that accompany the nitrospiropyran/merocyanine interconversion and relying instead solely on the intrinsically fast opening and closing of an oxazine ring. In fact, these structural modifications decrease the time required to complete a full switching cycle from hundreds of seconds to a few nanoseconds and increase the number of switching cycles, tolerated by the photochromic system, from a few tens to several thousands. Furthermore, the attachment of an appropriate chromophoric appendage to the oxazine heterocycle translates into the appearance of an intense absorption band in the visible region upon photoinduced ring opening. This absorption can be engineered to overlap the emission of a covalently connected borondipyrromethene and encourage the transfer of energy upon excitation. As a result, this structural design allows the modulation of fluorescence on the microsecond timescale for hundreds of switching cycles simply by opening and closing the oxazine ring under optical control. However, the ratio between the emission intensities of the two interconverting states, achieved at moderate illumination intensities, is relatively small because of the modest quantum efficiency of the photochromic transformation. The structural design of the fluorophore−photochrome dyad can be adjusted, yet again, to photoactivate, rather than photodeactivate, fluorescence and ensure a virtually infinite contrast ratio. In particular, the photoinduced generation of a chromophoric fragment that is able to absorb in the visible region can also be exploited to activate fluorescence, if the very same fragment is designed to be fluorescent. Specifically, the covalent connection of a coumarin fluorophore to an oxazine ring allows the photoinduced activation of fluorescence with a pair of beams designed to switch the photochromic component and excite the fluorescent one. Under these conditions, fluorescence turns on against a dark background and can be modulated on a microsecond timescale for hundreds of switching cycles. In principle, this unique behavior can be exploited to overcome diffraction with appropriate multiphoton illumination protocols and temporally resolve spatially indistinguishable fluorophores. Thus, the photochemical and photophysical properties of our compounds, coupled to their synthetic accessibility, can ultimately lead to the development of an entire family of photoswitchable fluorophores for super-resolution imaging. However, a further understanding of their excitation dynamics is essential to identifying viable strategies to enhance the quantum efficiency of the photoinduced ring-opening process, the brightness of the fluorescent state, and the ratio between the emission intensities of the two interconverting isomers. In this context, ultrafast spectroscopic analyses and electronic structure calculations will contribute to the elucidation of the stereoelectronic factors governing the properties of our molecular switches and guide our future structural designs.

■ ASSOCIATED CONTENT

Supporting Information. Steady-state absorption spectra of **8a**−**12a**. Time-resolved absorption spectra of **8a** and **10a**−**12a**. Temporal absorbance evolutions of **19a** and **25a** upon excitation. This material is available free of charge via the Internet at http://pubs.acs.org.

■ AUTHOR INFORMATION

Corresponding Author

*E-mail: ssortino@unict.it; fraymo@miami.edu.

■ ACKNOWLEDGMENT

We thank the National Science Foundation (CAREER Award CHE-0237578 and CHE-0749840) and the University of Miami for financial support.

■ REFERENCES

(1) Lakowicz, J. R. *Principles of Fluorescence Spectroscopy*; Springer: New York, 2006.

(2) Murphy, D. B. *Fundamentals of Light Microscopy and Electronic Imaging*; Wiley-Liss: New York, 2001.

(3) Pawley, J. B., Ed.; *Handbook of Biological Confocal Microscopy*; Springer: New York, 2006.

(4) Born, M.; Wolf, E. *Principles of Optics*; Cambridge University Press: Cambridge, U.K., 2002.
(5) Fernández-Suárez, M.; Ting, A. Y. *Nat. Rev. Mol. Cell. Biol.* **2008**, *9*, 929–943.
(6) Huang, B.; Bates, M.; Zhuang, X. *Annu. Rev. Biochem.* **2009**, *78*, 993–1016.
(7) Hell, S. W. *Nat. Methods* **2009**, *6*, 24–32.
(8) Heilemann, M.; Dedecker, P.; Hofkens, J.; Sauer, M. *Laser Photon Rev.* **2009**, *3*, 180–202.
(9) Toomre, D.; Bewersdorf, J. *Annu. Rev. Cell Dev. Biol.* **2010**, *26*, 285–314.
(10) Vogelsang, J.; Steinhauer, C.; Forthmann, C.; Stein, I. H.; Person-Skergo, B.; Cordes, T.; Tinnefeld, P. *ChemPhysChem* **2010**, *11*, 2475–2490.
(11) Thompson, M. A.; Biteen, J. S.; Lord, S. J.; Conley, N.; Moerner, W. E. *Methods Enzymol.* **2010**, *475*, 27–59.
(12) Cusido, J.; Impellizzeri, S.; Raymo, F. M. *Nanoscale* **2011**, *3*, 59–70.
(13) Dorion, G. H.; Wiebe, A. F. *Photochromism*; Focal Press: New York, 1970.
(14) Brown, G. H., Ed. *Photochromism*; Wiley: New York, 1971.
(15) El'tsov, A. V., Ed. *Organic Photochromes*; Consultants Bureau: New York, 1990.
(16) Bouas-Laurent, H., Dürr, H., Eds. *Photochromism: Molecules and Systems*; Elsevier: Amsterdam, 1990.
(17) Crano, J. C., Guglielmetti, R., Eds. *Organic Photochromic and Thermochromic Compounds*; Plenum Press: New York, 1999.
(18) Irie, M. *Chem. Rev.* **2000**, *100*, 1683–1890.
(19) Kuz'min, M. G.; Koz'menko, M. V. In *Organic Photochromes*; El'tsov, A. V., Ed.; Consultants Bureau: New York, 1990; pp 245−265.
(20) (a) Raymo, F. M.; Tomasulo, M. *Chem. Soc. Rev.* **2005**, *34*, 327–336. (b) Raymo, F. M.; Tomasulo, M. *J. Phys. Chem. A* **2005**, *109*, 7343–7352. (c) Cusido, J.; Deniz, E.; Raymo, F. M. *Eur. J. Org. Chem.* **2009**, 2031–2045. (d) Yildiz, I.; Deniz, E.; Raymo, F. M. *Chem. Soc. Rev.* **2009**, *38*, 1859–1867.
(21) Gross, H.; Dürr, H.; Retting, W. *J. Photochem.* **1984**, *26*, 165–178.
(22) Görner, H.; Fischer, C.; Gierisch, S.; Daub, J. *J. Phys. Chem.* **1993**, *97*, 4110–4117.
(23) Weber, C.; Rustemeyer, F.; Dürr, H. *Adv. Mater.* **1998**, *10*, 1348–1351.
(24) Sheepwash, M.; Mitchell, R. H.; Bohne, C. *J. Am. Chem. Soc.* **2002**, *124*, 4693–4700.
(25) Liang, Y.; Dvornikov, A. S.; Rentzepis, P. M. *J. Mater. Chem.* **2003**, *13*, 286–290.
(26) Myles, A. J.; Branda, N. R. *J. Am. Chem. Soc.* **2001**, *123*, 177–178.
(27) Straight, S. D.; Andréasson, J.; Kodis, G.; Bandyopadhyay, S.; Mitchell, R. H.; Moore, T. A.; Moore, A. L.; Gust, D. *J. Am. Chem. Soc.* **2005**, *127*, 9403–9409.
(28) Liu, L.-H.; Nakatani, K.; Pansu, R.; Vachon, J.-J.; Tauc, P.; Ishow, E. *Adv. Mater.* **2007**, *19*, 433–436.
(29) Berberich, M.; Krause, A.-M.; Orlandi, M.; Scandola, F.; Würthner, F. *Angew. Chem., Int. Ed.* **2008**, *47*, 6616–6619.
(30) Bahr, J. L.; Kodis, G.; de la Garza, L.; Lin, S.; Moore, A. L.; Moore, T. A.; Gust, D. *J. Am. Chem. Soc.* **2001**, *123*, 7124–7133.
(31) Myles, A.; Branda, N. R. *Adv. Funct. Mater.* **2002**, *12*, 167–173.
(32) Giordano, L.; Jovin, T. M.; Irie, M.; Jares-Erijman, E. A. *J. Am. Chem. Soc.* **2002**, *124*, 7481–7489.
(33) Harbron, E. J.; Vicente, D. A.; Hoyt, M. T. *J. Phys. Chem. B* **2004**, *108*, 18789–18792.
(34) Bossi, M.; Belov, V.; Polyakova, S.; Hell, S. W. *Angew. Chem., Int. Ed.* **2006**, *45*, 7462–7465.
(35) Jukes, R. T.; Adamo, V.; Hartl, F.; Belser, P.; De Cola, L. *Inorg. Chem.* **2004**, *43*, 2779–2792.
(36) The operating principles for fluorescence switching with photochromic compounds are reviewed in ref 20. Representative examples of these mechanisms in action are reported in refs 21−35.
(37) (a) Bertelson, R. C. In *Photochromism*; Brown, G. H., Ed.; Wiley: New York, 1971; pp 45−431. (b) Bertelson, R. C. In *Organic Photochromic and Thermochromic Compounds*; Crano, J. C., Guglielmetti, R., Eds.; Plenum Press: New York, 1999; Vol. 1, pp 11−83.
(38) Kholmanskii, A. S.; Dyumanev, K. M. *Russ. Chem. Rev.* **1987**, *56*, 136–151.
(39) Guglielmetti, R. In *Photochromism: Molecules and Systems*; Dürr, H., Bouas-Laurent, H., Eds.; Elsevier: Amsterdam, 1990; pp 314−466 and 855−878.
(40) (a) Ichimura, K. In *Photochromism: Molecules and Systems*; Dürr, H., Bouas-Laurent, H., Eds.; Elsevier: Amsterdam, 1990; pp 903−918. (b) Ichimura, K.; Seki, T.; Kawamishi, Y.; Suzuki, Y.; Sakuragi, M.; Tamaki, T. In *Photo-Refractive Materials for Ultrathin Density Optical Memory*; Irie, M., Ed.; Elsevier: Amsterdam, 1994; pp 55−83. (c) Ichimura, K. In *Photochromic Polymers*; Crano, J. C., Guglielmetti, R., Eds.; Plenum Press: New York, 1999; Vol. 2, pp 9−63. (d) Ichimura, K. *Chem. Rev.* **2000**, *100*, 1847–1873.
(41) Crano, J. C.; Kwak, W. S.; Welch, C. N. In *Applied Photochromic Polymer Systems*; McArdle, C. B., Ed.; Blackie: Glasgow, 1992; pp 31−79.
(42) (a) Krongauz, V. In *Applied Photochromic Polymer Systems*; McArdle, C. B., Ed.; Blackie: Glasgow, 1992; pp 121−173. (b) Berkovic, G.; Krongauz, V.; Weiss, V. *Chem. Rev.* **2000**, *100*, 1741–1754.
(43) Irie, M. In *Applied Photochromic Polymer Systems*; McArdle, C. B., Ed.; Blackie: Glasgow, 1992; pp 174−206.
(44) Hibino, J.; Hashida, T.; Suzuki, M. In *Photo-Refractive Materials for Ultrathin Density Optical Memory*; Irie, M., Ed.; Elsevier: Amsterdam, 1994; pp 25−53.
(45) Kawata, S.; Kawata, Y. *Chem. Rev.* **2000**, *100*, 1777–1788.
(46) Delaire, J. A.; Nakatani, K. *Chem. Rev.* **2000**, *100*, 1817–1845.
(47) Tamai, N.; Miyasaka, H. *Chem. Rev.* **2000**, *100*, 1875–1890.
(48) Minkin, V. I. *Chem. Rev.* **2004**, *104*, 2751–2776.
(49) (a) Tomasulo, M.; Deniz, E.; Alvarado, R. J.; Raymo, F. M. *J. Phys. Chem. C* **2008**, *112*, 8038–8045. (b) Deniz, E.; Tomasulo, M.; DeFazio, R. A.; Watson, B. D.; Raymo, F. M. *Phys. Chem. Chem. Phys.* **2010**, *12*, 11630–11634.
(50) (a) Atabekyan, L. S.; Chibisov, A. K. *Zh. Prikl. Spektrosk.* **1987**, *46*, 651–654. (b) Görner, H.; Atabekyan, L. S.; Chibisov, A. K. *Chem. Phys. Lett.* **1996**, *260*, 59–64. (c) Görner, H. *Chem. Phys.* **1997**, *222*, 315–329. (d) Chibisov, A. K.; Görner, H. *J. Photochem. Photobiol., A* **1997**, *105*, 261–267. (e) Chibisov, A. K.; Görner, H. *J. Phys. Chem. A* **1997**, *101*, 4305–4312. (f) Görner, H. *Chem. Phys. Lett.* **1998**, *282*, 381–390. (g) Görner, H. *Phys. Chem. Chem. Phys.* **2001**, *3*, 416–423.
(51) (a) Krysanov, S. A.; Alfimov, M. V. *Chem. Phys. Lett.* **1982**, *91*, 77–80. (b) Krysanov, S. A.; Alfimov, M. V. *Laser Chem.* **1984**, *4*, 129–138.
(52) Kalisky, Y.; Orlowski, T. E.; Williams, D. J. *J. Phys. Chem.* **1983**, *87*, 5333–5338.
(53) (a) Ito, T.; Hiramatsu, M.; Hirano, I.; Ohtani, H. *Macromolecules* **1990**, *23*, 4528–4532. (b) Ito, T.; Hiramatsu, M.; Hosoda, M.; Tsuchiya, Y. *Rev. Sci. Instrum.* **1991**, *62*, 1415–1419.
(54) Ernsting, N. P.; Arthen-Engeland, T. *J. Phys. Chem.* **1991**, *95*, 5502–5509.
(55) Quenching and sensitization experiments, coupled to the investigation of the photoinduced reisomerization of the colored isomers, demonstrate the fundamental role of T_1 in the photoisomerization of nitrospiropyrans.[50] Earlier reports, however, suggest alternative mechanisms for these photoinduced transformations. See refs 51−53 and (a) Irie, M.; Menju, A.; Hayashi, K. *Macromolecules* **1979**, *12*, 1176–1180. (b) Krongauz, V.; Kiwi, J.; Grätzel, M. *J. Photochem.* **1980**, *13*, 89–97. (c) Kalisky, Y.; Williams, D. J. *Macromolecules* **1984**, *17*, 292–296. (d) Lenoble, C.; Becker, R. S. *J. Phys. Chem.* **1986**, *90*, 62–65. (e) Tamaki, T.; Sakuragi, M.; Ichimura, K.; Aoki, K. *Chem. Phys. Lett.* **1989**, *161*, 23–26.
(56) Malkin, Ya. N.; Krasieva, T. B.; Kuzmin, V. A. *J. Photochem. Photobiol., A* **1989**, *49*, 75–88.
(57) Sakuragi, M.; Aoki, K.; Tamaki, T.; Ichimura, K. *Bull. Chem. Soc. Jpn.* **1990**, *63*, 74–79.

(58) Salemi, C.; Giusti, G.; Guglielmetti, R. *J. Photochem. Photobiol., A* **1995**, *86*, 247–252.
(59) Sheng, Y.; Leszcynski, J.; Garcia, A. A.; Rosario, R.; Gust, D.; Springer, J. *J. Phys. Chem. B* **2004**, *108*, 16233–16243.
(60) (a) Raymo, F. M.; Giordani, S. *J. Am. Chem. Soc.* **2001**, *123*, 4651–4652. (b) Raymo, F. M.; Giordani, S.; White, A. J. P.; Williams, D. J. *J. Org. Chem.* **2003**, *68*, 4158–4169.
(61) (a) Tomasulo, M.; Sortino, S.; Raymo, F. M. *Org. Lett.* **2005**, *7*, 1109–1112. (b) Tomasulo, M.; Sortino, S.; White, A. J. P.; Raymo, F. M. *J. Org. Chem.* **2005**, *70*, 8180–8189. (c) Tomasulo, M.; Sortino, S.; Raymo, F. M. *Asian Chem. Lett.* **2007**, *11*, 219–222.
(62) In principle, the nitro group of **6a** can facilitate intersystem crossing, as observed for **1a**. Nonetheless, the lifetime of T_1 associated with the 4-nitrophenoxy chromophore of **6a**, if at all formed, is presumably too short to sensitize significant amounts of singlet oxygen. Indeed, T_1 of 4-nitroanisole has a subnanosecond lifetime in acetonitrile (Mir, M.; Jansen, L. M. G.; Wilkinson, F.; Bourdelande, J. L.; Marquet, J. *J. Photochem. Photobiol., A* **1998**, *113*, 113–117).
(63) Photochromic oxazine **6a** can be trapped within poly(methyl methacrylate) films[61b] and attached covalently to hydrophobic (Tomasulo, M.; Deniz, E.; Benelli, T.; Sortino, S.; Raymo, F. M. *Adv. Funct. Mater.* **2009**, *19*, 3956−3961) or hydrophilic (Tomasulo, M.; Deniz, E.; Sortino, S.; Raymo, F. M. *Photochem. Photobiol. Sci.* **2010**, *9*, 136−140) polymers. The photochemical properties of the resulting materials are similar to those observed for **6a** in acetonitrile. However, the S_0 absorption, associated with the 4-nitrophenolate chromophore of the photogenerated species, decays biexponentially on a microsecond timescale under these conditions.
(64) (a) Tomasulo, M.; Raymo, F. M. *Org. Lett.* **2005**, *7*, 4633–4636. (b) Tomasulo, M.; Sortino, S.; White, A. J. P.; Raymo, F. M. *J. Org. Chem.* **2006**, *71*, 744–753. (c) Åxman Petersen, M.; Deniz, E.; Brøndsted Nielsen, M.; Sortino, S.; Raymo, F. M. *Eur. J. Org. Chem.* **2009**, 4333–4339.
(65) (a) Tomasulo, M.; Sortino, S.; Raymo, F. M. *Adv. Mater.* **2008**, *20*, 832–835. (b) Tomasulo, M.; Sortino, S.; Raymo, F. M. *J. Org. Chem.* **2008**, *73*, 118–126. (c) Tomasulo, M.; Sortino, S.; Raymo, F. M. *J. Photochem. Photobiol., A* **2008**, *200*, 44–49. (d) Deniz, E.; Tomasulo, M.; Sortino, S.; Raymo, F. M. *J. Phys. Chem. C* **2009**, *113*, 8491–8497.
(66) Oxazine **20a** switches to corresponding zwitterionic isomer **20b** upon ultraviolet illumination.[61b,61c] The quantum yield for the photoinduced ring-opening process is 0.03 (ϕ in Table 1), and the lifetime of the photogenerated isomer is 22 ns (τ in Table 1). The photochemical properties of this compound are also reported in Barkauskas, M.; Martynaitis, V.; Shachkus, A. A.; Rotomskis, R.; Sirutkaitis, V.; Vengris, M. *Lith. J. Phys.* **2008**, *48*, 231–242.
(67) The synthesis of **20a** was originally reported in (a) Shachkus, A. A.; Degutis, J.; Jezerskaite, A. In *Chemistry of Heterocyclic Compounds*; Kovac, J., Zalupsky, P., Eds.; Elsevier: Amsterdam, 1987; Vol. 35, pp 518−520. (b) Shachkus, A. A.; Degutis, J.; Urbonavichyus, A. G. *Khim. Geterotskil. Soed.* **1989**, *5*, 672–676. (c) *Chem. Heterocycl. Compd.* **1989**, 562–565.
(68) The introduction of an electron-withdrawing fluorine substituent in the para position, relative to the nitrogen atom, of the 2*H*,3*H*-indole fragment of **6a**[65d] and **19a** (Deniz, E.; Impellizzeri, S.; Sortino, S.; Raymo, F. M. *Can. J. Chem.* **2011**, *89*, 110−116) enhances the quantum efficiency of the photoinduced ring-opening process. By contrast, the attachment of an electron-donating methoxy group in the very same position prevents the photochemical transformation. These observations indicate that the quantum efficiency of the photoinduced ring-opening process is sensitive to the electron density on the nitrogen atom of the 2*H*,3*H*-indole fragment. Presumably, the transfer of one electron from this atom to the nitro group on the phenoxy chromophore upon excitation competes with the cleavage of the [C−O] bond required to open the oxazine ring.
(69) The $S_0 \rightarrow S_1$ absorption of the 3*H*-indolium cation of **14b** is centered at ca. 340 nm.[65d]
(70) The coloration efficiency of **15b** is lower than that of parent system **6b** because of the poor quantum yield for its photoinduced formation.[65d]
(71) The attachment of the 2-(4-(2-phenylethynyl)phenyl)ethynyl substituent of **18a** to the para position, relative to the nitrogen atom, of the 2*H*,3*H*-indole fragment rather than to the chiral center at the junction of the two heterocycles prevents ring opening.[65b] Instead of the S_0 absorption of the 4-nitrophenolate anion of the ring-open isomer, the time-resolved absorption spectrum of the resulting oxazine reveals a band at 510 nm. This band resembles the T_1 absorption of phenylvinylstilbene (Hara, M.; Samori, S.; Xichen, C.; Fujitsuka, M.; Majima, T. *J. Org. Chem.* **2005**, *70*, 4370−4374) and decays monoexponentially on a microsecond timescale. Thus, intersystem crossing dominates the excitation dynamics of this particular system.
(72) (a) Deniz, E.; Sortino, S.; Raymo, F. M. *J. Phys. Chem. Lett.* **2010**, *1*, 1690–1693. (b) Deniz, E.; Ray, S.; Tomasulo, M.; Impellizzeri, S.; Sortino, S.; Raymo, F. M. *J. Phys. Chem. A* **2010**, *114*, 11567–11575.
(73) Deniz, E.; Sortino, S.; Raymo, F. M. *J. Phys. Chem. Lett.* **2010**, *1*, 3506–3509.